

# Out-Clinic Pulmonary Disease Evaluation via Acoustic Sensing and Multi-task Learning on Commodity Smartphones

Xiangyu Yin, Kai Huang, Erick Forno, Wei Chen, Heng Huang and Wei Gao University of Pittsburgh USA

### **ABSTRACT**

Pulmonary diseases, such as asthma and Chronic Obstructive Pulmonary Disease (COPD), constitute a major public health challenge. The disease symptoms, including airway obstruction and inflammation, usually result in changes in airway mechanical properties, such as the caliber and impedance of the airway. To measure such airway properties for disease evaluation and diagnosis purposes, pulmonary function tests (PFT) has been widely adopted. However, most existing PFT systems require expensive and cumbersome hardware that are impossible to be used out of clinic. To allow out-clinic continuous pulmonary disease evaluation, in this paper we present AWARE, a new sensing and AI system that supports accurate and reliable PFT using commodity smartphones. AWARE uses a smartphone to transmit acoustic signals and reconstructs the profile of human airway based on the analysis of reflected acoustic waves captured from the smartphone's microphone. The subject's pulmonary condition is then evaluated by a multi-task learning model that integrates both the airway measurements and the subject's lung function records as the ground truth. Evaluations on 75 human subjects demonstrate that AWARE has the capability to achieve 80% accuracy on distinguishing between humans with healthy pulmonary function and with asthma symptoms.

# **CCS CONCEPTS**

 $\bullet \mbox{ Human-centered computing} \rightarrow \mbox{Ubiquitous and mobile computing};$ 

### **KEYWORDS**

Pulmonary disease evaluation, acoustic sensing, smartphone, multitask learning

### **ACM Reference Format:**

Xiangyu Yin, Kai Huang, Erick Forno, Wei Chen, Heng Huang and Wei Gao. 2022. Out-Clinic Pulmonary Disease Evaluation via Acoustic Sensing and Multi-task Learning on Commodity Smartphones. In *The 20th ACM Conference on Embedded Networked Sensor Systems (SenSys '22), November 6–9, 2022, Boston, MA, USA.* ACM, New York, NY, USA, 7 pages. https://doi.org/10.1145/3560905.3568437

Permission to make digital or hard copies of all or part of this work for personal or classroom use is granted without fee provided that copies are not made or distributed for profit or commercial advantage and that copies bear this notice and the full citation on the first page. Copyrights for components of this work owned by others than the author(s) must be honored. Abstracting with credit is permitted. To copy otherwise, or republish, to post on servers or to redistribute to lists, requires prior specific permission and/or a fee. Request permissions from permissions@acm.org.

SenSys '22, November 6–9, 2022, Boston, MA, USA
© 2022 Copyright held by the owner/author(s). Publication rights licensed to ACM.
ACM ISBN 978-1-4503-9886-2/22/11...\$15,00

https://doi.org/10.1145/3560905.3568437

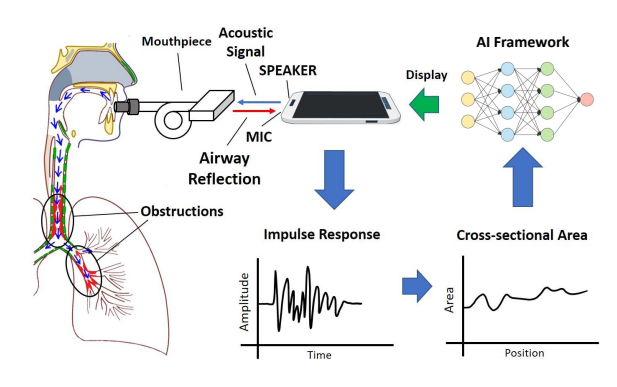


Figure 1: Overall picture of AWARE

#### 1 INTRODUCTION

Pulmonary diseases constitute a major public health challenge [3]. For example, over 330 million people worldwide have asthma, including 25 million in the US [5]. Chronic obstructive pulmonary disease (COPD) affects another 16 million people in the US. Emerging pulmonary diseases, such as H1N1 swine flu and COVID-19, have also made and been making catastrophic impacts on society. Pulmonary diseases produce symptoms such as airway inflammation [4, 6] and mucus hypersecretion [8], which result in airway obstruction [9, 23] and changes in airway mechanical properties, such as caliber and impedance.

For disease evaluation purposes, Pulmonary Function Testing (PFT) is used as the objective evaluation of such airway mechanical changes. In particular, humans with pulmonary diseases usually suffer from frequent disease exacerbations that cause emergency room visits, hospitalizations, and sometimes death. Continuous PFT out of clinic, hence, is critical for disease monitoring, diagnosis and management [24]. However, most of current PFT methods [7, 22, 26] require cumbersome hardware that are unavailable out of clinic. Some recent research efforts reduce the hardware size, but their costs (>\$2,000) are too high to be used out of clinic [21]. Low-cost PFT devices priced at <\$100 [1, 2], on the other hand, have low accuracy and could produce >20% measurement error [16].

In this paper, we present AWARE (Acoustic WAveform Respiratory Evaluation), a new system design that uses commodity smartphones to bridge the gap between current clinical PFTs and the great need of PFT out of clinic. As shown in Figure 1, our design uses the smartphone's speakers and microphones to build an acoustic sensing system, which probes the profile of airway from the reflected acoustic signal in the form of cross-sectional area (CSA) at different airway positions. The airway profile, then, is used as the input to a multi-task deep learning model, which provides prediction of pulmonary disease conditions and lung function indices.





(a) Impulse Oscillometry System (IOS)

(b) Acoustic Reflection Technique (ART)

Figure 2: Clinical devices of IOS and ART

### 2 RELATED WORK

It has been proved that acoustic methods could be useful tools for measuring human airway conditions, such as narrowing and obstruction. One of these methods is the forced oscillation technique (FOT) [22]. Sinusoidal pressure waves ranging from 5 to 30Hz are generated by loudspeaker transmitted into the lungs. The overall impedance of airway is then determined by measuring the magnitude of changes in pressure and flow, which will be used to identify possible airway obstruction or narrowing. An advanced version of FOT called impulse oscillometry system (IOS) uses pulses as the transmitted signal to achieve better frequency-domain resolution [7]. Another acoustic method that aims to provide more detailed information is the acoustic reflection technique (ART) [13], also known as airway area by acoustic reflection (AAAR) [10, 14] or acoustic pharyngometry (APh) [20]. Instead of directly calculating the overall impedance from pressure and airflow change in airway, this technique gives an estimation of cross-sectional area over different positions in the airway.

In practice, however, these techniques are limited to in-clinic use due to the cumbersome devices they need, as shown in Figure 2. The subject is also instructed to do several exhale tasks for data acquisition. On the other hand, smartphone-based sensing systems were introduced in the past few years. Typical spirometer-like approaches require expensive external sensing hardware that are attached to the smartphone via cable, WiFi, or Bluetooth [1, 29]. Other acoustic sensing approaches leverage smartphones' built-in microphones to passively overhear the breathing sounds and give lung function predictions [11, 15, 30], but cannot provide detailed information about the airway's physiological conditions. In contrast, our sensing approach provides highly accurate measurements of the airway's internal conditions, in an non-invasive and effortless manner without using any extra hardware.

# 3 ACOUSTIC SENSING FOR AIRWAY MEASUREMENT

In this section, we introduce our technique of measuring human airway by acoustic reflections using smartphones, especially how to overcome the hardware constraints when adopting acoustic reflection technique (ART) onto smartphones.

## 3.1 Preliminaries

To estimate airway mechanical condition in a non-invasive manner, AWARE adopts the existing acoustic reflection technique (ART), which reconstruct the airway CSA based on the analysis of airway's acoustic reflection properties [10, 14, 18]. To do so, AWARE

transmits a series of acoustic pulses through the smartphone's bottom speaker into the airway, and records the reflected signal using smartphone's microphone. With both the transmitted and received signal, AWARE can derive the impulse response (IR) of human airway and convert the IR into CSA measurement.

The key challenge is the smartphone's hardware constraints, including the poor low-frequency performance of the speaker and inappropriate layout of bottom speaker and microphone. First, the smartphone's speakers are designed for routine use rather than sensing, and thus only have high gain from 200Hz to 10000Hz [27]. However, the algorithm of ART is quite sensitive to low-frequency components (<200Hz). Hence, minimizing the error that is brought by low-frequency noise becomes is crucial.

In a traditional ART system, the speaker and microphone are placed far away from each other (>50cm), in order to unmix the extra echoes called source reflection [17, 25]. However, in a smartphone set-up, the speaker and microphone are usually very close to each other, hence bringing a challenge to deal with the unnecessary source reflection. AWARE uses extra calibration steps and newly developed algorithms to eliminate the impact of source reflection.

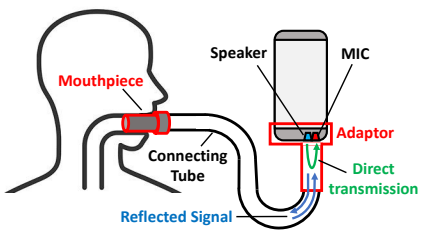


Figure 3: Sensing system design for airway measurement

### 3.2 Sensing System Design

As shown in Figure 3, AWARE is a smartphone-based system that consists of an Android app, a plastic phone adapter, a soft probing tube, and a 3D-printed plastic mouthpiece. To use AWARE, as shown in Figure 4, one handholds the smartphone connected to the probing tube, bites on the mouthpiece, and breath through the tube. AWARE transmits a series of acoustic pulses through the bottom speaker and analyze the reflected signal received by the microphone.



Figure 4: An example of using AWARE

When the acoustic wavelength is larger than the airway diameter, it is appropriate to consider an one-dimension plane-wave propagation of the acoustic pressure wave. Such 1-D plane-wave will be partially reflected when it encountered an impedance change within the duct-like airway, while the cross-sectional area (CSA) is the major determining factor of the impedance in our case. Therefore, by inversely calculating the reflection coefficient from the received

signal, an area-distance curve is eventually given to indicate the CSA at different positions within the airway.

3.2.1 Calibration and Data Collection. Considering the heterogeneity of smartphone speakers and microphones, as well as the manufacturing error of adapter, tube and mouthpiece, the data collected from different devices could largely vary. To remove such impact of different hardware, a three-step calibration is conducted before the data from testing subject is collected.

In the first step, a much longer probing tube is used instead of the short tube being used in CSA measurements. This tube is considered as a semi-infinite tube since it is long enough to avoid noticeable reflection from the end. Pure "direct transmission" is collected in this case, which refers to the signal that directly propagates from the speaker to the microphone. In the second and third step, the short tube is placed, and data is collected without the testing subject (user's airway) involved. The outlet of the tube is kept open in the second step and blocked by hand in the third step. Standard reflected signal is collected in these two cases.

After the calibration phase is finished, testing subject is coupled to the probing tube. In this subject testing phase, AWARE collects reflected signal that comes from the subject and send it together with the calibration signals to the signal processing program.

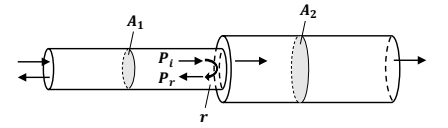
3.2.2 Airway Profile Reconstruction. Sharing the same principle as ART, AWARE takes two steps to reconstruct the profile of airway: acquisition of impulse response and reconstruction of CSA. The signal processing program first deconvolutes the signal collected in subject testing phase by the direct transmission collected in first step of calibration. By doing so, the impulse response of the airway system is obtained. Impulse response is defined as the output of a dynamic system when the input is an ideal impulse, thus can be used to indicates the characteristics of the airway system.

Given the impulse response, it is possible to recover the reflection coefficient of different position within the airway, and therefore reconstruct the CSA. Suppose an ideal impulse signal was transmitted into the airway and propagate as a 1-D plane-wave. The impulse will be reflected wherever a CSA change exists. The farther and larger the change is, the later and stronger the reflected impulse is received. This principle gives a possibility to inversely calculate how much and where the CSA changes from the impulse response.

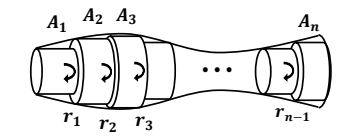
However, considering that human airway is a duct with continuously varying CSA, the actual case becomes much more complicated. The signal could bounce around in the airway and the actual received signal is a mixture of infinite reflections. Fortunately, Ware and Aki [28] provided a layer-peeling procedure to recursively calculate CSA changes from near to far. The detailed solution is described in Section 3.3.

3.2.3 Source Reflection Removal. The standard ART procedure works perfectly when microphone is far away from the speaker. However, when ART is applied to smartphone, the speaker and microphone are usually very close to each other, leading to the problem of source reflection. The source reflection means that the reflected signal from subject will be reflected again by the surface of smartphone, and be recorded by the microphone again. When speaker and microphone are close, the main and source reflected signal will be overlapped.

We solve this problem by abstracting the phenomenon into a frequency-domain infinite series and use calibration data to derive the parameters in the series. Such parameters represent the characteristics of source reflection and signal decay, thus can be used to remove the impact of source reflection when calculating the true impulse response. Details are elaborated in Section 3.4.



(a) Modeling of A simple two-segment case



(b) Modeling of continuous varying cross-sectional area

Figure 5: Sound propagation model in duct

# 3.3 Airway Profile Reconstruction

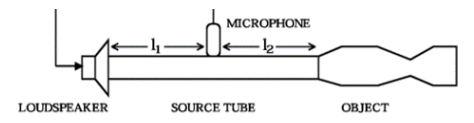
In this subsection, we introduce the two steps used in ART for airway profile reconstruction: acquisition of impulse response and reconstruction of cross-sectional area.

3.3.1 Acquisition of Impulse Response. To acquire the impulse response of the subject, AWARE applies standard frequency-domain deconvolution. The Fourier transform of the incident and reflected signals are computed and divided to estimate the frequency response of airway. The impulse response is then obtained by inverse Fourier transform of the frequency response. To achieve accurate estimation, the spectrum of the transmitted signal should not miss any frequency components across the entire bandwidth. Impulse signal is a good choice because it mathematically has a flat and complete spectrum. However, in practice, there is no way for a speaker to generate an ideal impulse. Thus, approximate pulses with short duration are used as alternatives.

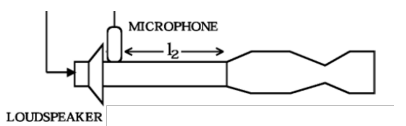
3.3.2 Reconstruction of Cross-sectional Area. The backbone of the reconstruction relies on the assumption that low-frequency acoustic signals (approximately below 10kHz) travel as 1-D plane wave along human airway. Under such assumption, the airway could be considered as a duct with continuously varying cross-sectional area. When an acoustic wave travels along a duct and encounter a cross-sectional area change, it will be partially reflected. A simple example is the two-segment case shown in Figure 5a. Therefore, the relative change of cross-sectional area can be obtained by measuring the ratio of reflected and incident wave  $P_r/P_i$ , namely the reflection coefficient r, using following equation:  $A_2/A_1 = (1-r)/(1+r) = (1-P_r/P_i)/(1+P_r/P_i)$ .

Then, for a duct with arbitrary shape, the general idea is to divide it into multiple small segments with constant length and cross-sectional area  $A_1$  to  $A_n$ , as shown in Figure 5b. However, due to multiple reflections between different segments, actual analysis of the model is not simple. In general, the Z-transform of the impulse response  $H(z) = \mathcal{Z}\{h(t)\}$  has the following relationship with reflection coefficients  $r_1, r_2 \dots r_{n-1}$ :

$$\begin{bmatrix} H(z) \\ 1 \end{bmatrix} = Q_1 Q_2 \dots Q_{n-1} \begin{bmatrix} 0 \\ T(z) \end{bmatrix}$$
 (1)



(a) A standard ART configuration



(b) A smartphone-based configuration

Figure 6: ART sensing system configuration

where

$$Q_k = \frac{1}{1 + r_k} \begin{bmatrix} z^{-1/2} & r_k z^{1/2} \\ r_k z^{-1/2} & z^{1/2} \end{bmatrix}$$
 (2)

and T(z) is an intermediate variable that can be jointly solved with H(z). H(z) can be further expanded as

$$H(z) = H_1 z^{-1} + H_2 z^{-2} + H_3 z^{-3} + \dots$$
 (3)

where  $H_1$  only depends on  $r_1$ ,  $H_2$  depends on  $r_1$  and  $r_2$ ,  $H_3$  depends on  $r_1$ ,  $r_2$  and  $r_3$ , etc. Similarly, every following  $r_k$  can be calculated given  $H_k$  and all previous r. Afterwards, the relative changes between two adjacent segments are derived from  $A_{k+1}/A_k = (1 - r_k)/(1 + r_k)$ . Such process provides the estimation of the cross-sectional areas of different positions in the duct, and an area-distance curve is eventually given.

## 3.4 Removing Source Reflection

In this subsection, we elaborate the challenge of source reflection and the approach to remove its impact.

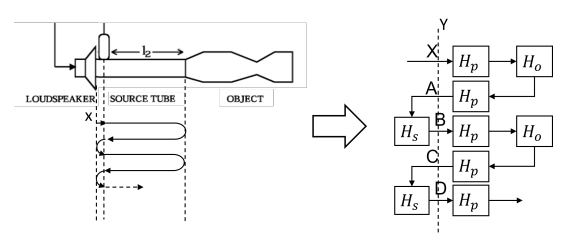


Figure 7: Modeling of Source Reflection

3.4.1 The Model of Source Reflection. In standard ART, the experimental setup is as shown in Figure 6a. The microphone is mounted onto the tube wall and is quite far away from the loud-speaker mounted at the tube end. Since the signal reflected by the subject will travel back through the tube and be reflected again by the sound source (the loudspeaker), the distance between microphone and speaker makes sure that the signal from subject is separated from any further source reflection.

However, under a smartphone setup, as shown in Figure 6b, the distance between speaker and microphone is pre-fixed and is insufficient for such separation. The source reflection is hence overlapped with the wanted signal. Such overlapping could lead to strong distortion to the impulse response.

Fortunately, under the 1-D plane-wave propagation model, all parts that create reflections can be described as LTI systems with a frequency response indicating the system properties. The impact of source reflection can be described using frequency response  $H_s$ . This means if a signal x coming towards the source has a Fourier Transform of X, the signal reflected by the source will have a Fourier Transform of  $H_sX$ . Similarly, we can also describe the propagation delay and signal decay together as a system with frequency response  $H_p$ , and the testing subject as a system with  $H_o$ . Following such denotation, the signal travel path can be abstracted using a block diagram shown in Figure 7. Assume the original transmitted signal is x with Fourier Transform being X, and the final signal received at the microphone is y with Fourier Transform being Y, the relationship between X and Y can be written as:

$$Y = X + A + B + C + D + \dots$$
  
=  $X + H_p^2 H_o X + H_p^2 H_s H_o X + H_p^4 H_s H_o^2 X + \dots$  (4)

Notice that this formula is actually an infinite geometric sequence, so the equation can be further written into:

$$Y = X(1 + H_p^2 H_o + H_p^2 H_s H_o + H_p^4 H_s H_o^2 + H_p^4 H_s^2 H_o^2 + \dots)$$
  
=  $X \cdot (1 + H_p^2 H_o) / (1 - H_p^2 H_s H_o).$  (5)

Now, the problem becomes how to get our true target  $H_o$ .

3.4.2 Calibration against Source Reflection. From Eq. (5), we notice that to get our target  $H_o$ , we must first know X, Y,  $H_s$ , and  $H_p$ . X and Y exactly correspond to the data we collected in first step of calibration phase and in subject testing phase, respectively. For  $H_s$  and  $H_p$ , however, we will need the data collected in the second and third step of calibration.

In second and third step of calibration, we measured the reflection of a pure "closed end" and a pure "open end". From the 1-D plane-wave propagation model, a "closed end" has  $H_0=1$  and an "open end" has  $H_0=-1$ . Denote the signal collected in these two steps as  $Y_1$  and  $Y_2$ , we can have such equations:

$$Y_1 = X \frac{1 + H_p^2}{1 - H_p^2 H_s}, Y_2 = X \frac{1 - H_p^2}{1 + H_p^2 H_s}$$
 (6)

Therefore, we can get

$$H_p^2 = \frac{(Y_1 + Y_2)X - 2Y_1Y_2}{(Y_1 - Y_2)X}, H_p^2 H_s = \frac{Y_1 + Y_2 - 2X}{Y_1 - Y_2}.$$
 (7)

By taking these two results into Eq. (5), we can then get the target  $H_o$ , and by taking the inverse Fast Fourier Transform of  $H_o$ , we can get target impulse response of the subject.

# 4 MULTI-TASK LEARNING FOR DISEASE EVALUATION

In this section, we describe how AWARE helps pulmonary disease evaluation using multi-task learning.

# 4.1 Design Rationale

With the airway CSA measurement, it is important to consider how to interpret such result and reveal its relationship to the pulmonary diseases. However, most existing research efforts have been focusing on discovering the correlation between airway CSA measurements and upper airway diseases like sleep apnea. It remains an uncharted territory to utilize this technique for pulmonary diseases evaluation such as asthma and COPD that mainly affect lower airways. On the other hand, spirometry, as the most commonly used PFT, has been the gold standard for pulmonary disease evaluation.

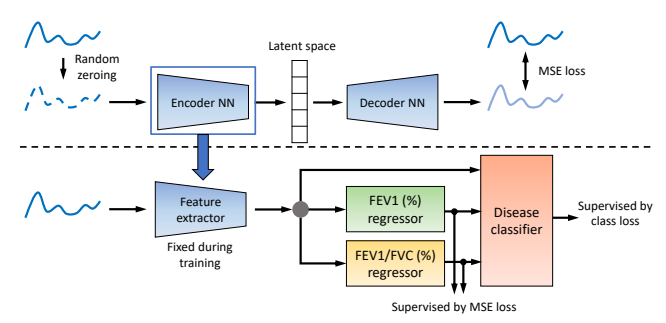


Figure 8: Multi-task Learning Model

Therefore, we come with the idea of building a multi-task learning framework which uses spirometry measurements to assist disease evaluation from airway CSA measurement.

As shown in Figure 8, our multi-task learning model consists of three major parts: 1) a feature extractor that takes the airway CSA measurement as input, 2) two regressors that estimate the lung function indices being used in spirometry, and 3) a classifier that gives prediction of the disease condition. The feature extractor is an encoder taken from an auto-encoder (AE) structure that is trained to extract the representative features from CSA measurements. It converts the CSA measurement into a 48-element feature array. The regressor then takes the features as the input and predict the lung function indices. After that, both the features and the predicted lung function indices are used as the input to the classifier, which gives the prediction of whether the patient has the disease.

### 4.2 Feature Extractor

To extract features from the airway CSA measurement, we train an auto-encoder with a 3-layer encoder and a 3-layer decoder, and use the encoder part as the feature extractor. The key challenge of training such an auto-encoder is the overfitting problem given limited amount of data collected in clinic. Therefore, before feeding the CSA measurements into the auto-encoder, we augment the input data by random zeroing to mitigate overfitting and to help the latent features better represent the underlying patterns of the CSA measurement curves. The mean-square error (MSE) between the recovered and original curve is used as the loss function for training. After training is finished, the encoder is extracted as the feature extractor that participate in predicting disease.

# 4.3 Regressors and Classifier for Disease Evaluation

In clinical diagnosis of asthma and COPD, several indices that obtained from spirometry are used. Spirometry mechanically measures the volume and velocity of the subject's airflow with forced expiration [19], and evaluates lung function in peak expiatory flow (PEF), forced expiratory volume in 1 second (FEV1) and forced vital capacity (FVC). However, the measurements of PEF, FEV1, and FVC are highly correlated with the subject's age, height, gender and race. Therefore, the actual metrics being used in clinic are the percentiles of PEF, FEV1, and FVC to the reference value[12]. Among all of the metrics, the most commonly used and reliable ones are the FEV1 and the ratio of FEV1 to FVC (FEV1/FVC).

In our model, two regressors take the extracted features of the airway CSA measurement as the input, and predict the subject's FEV1 and FEV1/FVC percentile, respectively. Each regressor consists of 3 fully connected layers, and the outputs are supervised by the MSE loss compared to the subject's clinical spirometry measurements being used as the ground truth. The predicted FEV1 and FEV1/FVC, together with the extracted features of the airway CSA measurement, are then used as the input to to a disease predictor. Such design builds on the basis that our acoustic sensing and spirometry provide two different modalities for measuring the airway mechanics that complement each other. With the regressors, we only need the subject's spirometry measurements during offline training. For inference stage, the only input to the model is the airway CSA measurement, and both the disease prediction and the predicted value of FEV1 and FEV1/FVC are given.

### 5 PERFORMANCE EVALUATION

We evaluated the accuracy of AWARE in different scenarios: 1) concatenated plastic tubes with different calibers; 2) 3D-printed human airway models with different scales; 3) human subjects.

# 5.1 Accuracy on Concatenated Tubes

To investigate the CSA measurement accuracy by acoustic sensing, we first conducted lab experiments in which the testing subjects are several sets of concatenated plastic tubes with various calibers. The tubes are directly connected to AWARE system's probing tube without the mouthpiece. Each case is tested 5 times and 25 probing pulses are transmitted in 5 seconds in each experiment. Mean absolute percentage error (MAPE) between the measured and the actual CSA of the tubes is calculated as:

MAPE = 
$$\frac{100\%}{n} \sum_{t=1}^{n} \left| \frac{A_t - A_p}{A_t} \right|$$
 (8)

where  $A_p$  is the measured CSA by AWARE and  $A_t$  is the actual CSA of the tube. As shown in Figure 9, AWARE can achieve an average error of 5-12% when measuring the CSA of different positions of the tube, and the results are highly repeatable.

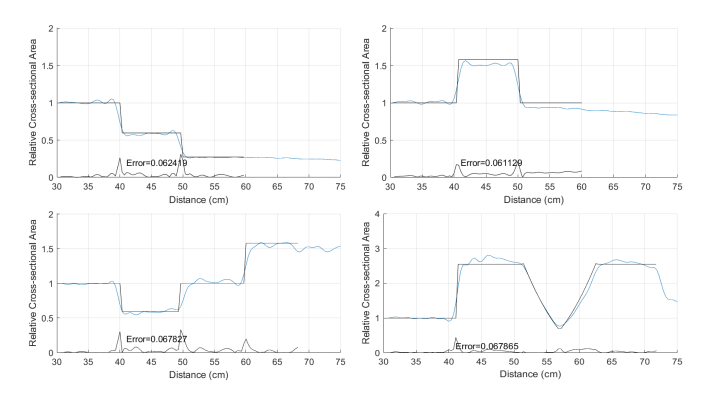


Figure 9: CSA measurements of concatenated tubes

# 5.2 Accuracy on 3D-printed Airway Models

To further evaluate AWARE's CSA measurement accuracy on ducts with more complicated shapes and its capability of detecting mechanical changes in the real human airway, we use 3D-printed human airway models with different scales. These airway models

are printed according to CT scan data from real human bodies. As shown in Figure 10, the airway model is composed of an upper airway part and a lower airway part, where the upper airway has a fixed size and the lower airway has three different scales: 100%, 90%, and 80%. The two parts are connected using a short plastic tube, and the openings of both parts are precisely designed to make sure the tube can be tightly plugged in.



Figure 10: Realistic airway models with different scales

In this setup, the ground truth of airway model's CSA is hard to measure, and so we measure AWARE's accuracy using the relative error between different scales. As shown in Figure 11, the curves for the airway segment between 0 and 18cm are quite consistent since they correspond to the upper airway model which has a fixed size. After 18cm, the curves are consistent with respect to the different scales of the models being used. For example, when measuring the length between first and second significant peak after 18cm (correspond to the length of main trachea), and the amplitude of second peak (correspond to the CSA of carina), the relative error is <3% compared to the 100%-scale model.

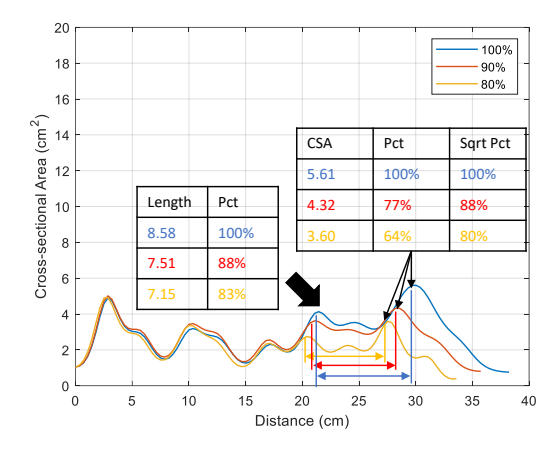


Figure 11: CSA measurement of realistic airway models

### 5.3 Clinical Study on Human Subjects

We also evaluated AWARE's measurement accuracy with a clinical study over 75 human subjects recruited through the Children's Hospital of Pittsburgh<sup>1</sup>. Among these human subjects, 39 of them are adults and 36 are below age 18. 46 of these subjects have been diagnosed as asthma patients in clinic, and the rest 29 are healthy.

The subjects were asked to use AWARE under the guidance of physicians in clinic, and also required to collect spirometry data afterwards. The subjects need to follow a detailed protocol to complete the AWARE tests, including 3 normal respiration cycles. Each

Table 1: Human Subjects' Information

Category	Characteristics	Number	
Demographics	Tests per subject	$2.98 \pm 1.24$	
	Age (years)	$25.19 \pm 17.60$	
	Adults (%)	39(52.0)	
	Female (%)	40(53.3)	
	Caucasian (%)	51(68.0)	
	African-American (%)	24(32.0)	
Body conditions	Height (cm)	$161.23 \pm 16.09$	
	Weight (kg)	$71.45 \pm 27.98$	
Pulmonary diseases	Asthma	46(61.3)	
	Healthy	29(38.7)	

inhalation or exhalation stage lasts for 5 seconds during which 25 probing acoustic pulses are transmitted in AWARE. The airway CSA measurements during exhalation stages were then averaged and used for evaluation. In total, 224 samples were collected and used to train the multi-task learning model. The multi-task learning model is expected to distinguish between asthma patients and healthy human subjects.

Group	Test-level accuracy	Subject-level accuracy
Adults	58.88%	75.67%
Minors	90.60%	84.21%
Overall	75.45%	80.00%

**Table 2: Disease Prediction Accuracy** 

The samples are divided into training and validation datasets using 5-fold cross-validation. The multi-task learning model is then trained based on such dataset division. Both test-level accuracy and subject-level accuracy are measured. As shown in Table 2, AWARE achieves 80% subject-level accuracy when predicting asthma patients over the whole subject group, and achieves 75.67% and 84.21% accuracy on adults and minors separately. The fact that the accuracy on minors are significantly higher than on adults are potentially because of the imbalanced labels in two groups. Only 12 out of 39 adults are asthma patients while the number is 34 out of 36 in minors. A more balanced dataset could help to address this issue.

### 6 CONCLUSION AND FUTURE WORK

In this paper, we present AWARE, a new sensing system which accurately measures human airway calibers and predict pulmonary disease conditions. Clinical study showed that AWARE can achieve 80% accuracy on predicting asthma symptoms. In the future, we will focus on new system designs to deal with different human factors such as unwanted tongue movements, breathing sound, and smartphone hardware heterogeneity. Such designs may involve new adapter and mouthpiece design and algorithm improvements.

## **ACKNOWLEDGMENTS**

We thank the anonymous reviewers for their comments and feedback. This work was supported in part by National Science Foundation (NSF) under grant number CNS-1812407, CNS-2029520, IIS-1956002, IIS-2205360, CCF-2217003 and CCF-2215042.

 $<sup>^1\</sup>mathrm{University}$  of Pittsburgh IRB approval No. STUDY20040181-01.

#### REFERENCES

- [1] 2022. MIR SmartOne. https://www.mirsmartone.com
- [2] Microlife AG. [n. d.]. PF 100 Asthma Monitor. https://www.microlife.com/ consumer-products/respiratory-care/digital-peak-flow-meter/pf-100
- [3] Katayoun Bahadori, Mary M Doyle-Waters, Carlo Marra, Larry Lynd, Kadria Alasaly, John Swiston, and Js Mark FitzGerald. 2009. Economic burden of asthma: a systematic review. BMC pulmonary medicine 9, 1 (2009), 1–16.
- [4] William W Busse, William F Calhoun, Julie D Sedgwick, et al. 1993. Mechanisms of airway inflammation in asthma. American Review of Respiratory Disease 147 (1993), S20–S20.
- [5] CDC. [n. d.]. Most Recent National Asthma Data. https://www.cdc.gov/asthma/most\_recent\_national\_asthma\_data.htm. August 3, 2021.
- [6] Robert Lorenz Chua, Soeren Lukassen, Saskia Trump, Bianca P Hennig, Daniel Wendisch, Fabian Pott, Olivia Debnath, Loreen Thürmann, Florian Kurth, Maria Theresa Völker, et al. 2020. COVID-19 severity correlates with airway epithelium-immune cell interactions identified by single-cell analysis. Nature biotechnology 38, 8 (2020), 970–979.
- [7] Koundinya Desiraju and Anurag Agrawal. 2016. Impulse oscillometry: the state-of-art for lung function testing. Lung India: official organ of Indian Chest Society 33, 4 (2016), 410.
- [8] Christopher M Evans, Kyubo Kim, Michael J Tuvim, and Burton F Dickey. 2009. Mucus hypersecretion in asthma: causes and effects. Current opinion in pulmonary medicine 15, 1 (2009), 4.
- [9] James E Fish and Stephen P Peters. 1999. Airway remodeling and persistent airway obstruction in asthma. *Journal of Allergy and Clinical Immunology* 104, 3 (1999), 509–516.
- [10] J. J. Fredberg, M. E. B. Wohl, G. M. Glass, and H. L. Dorkin. 1980. Airway area by acoustic reflections measured at the mouth. *Journal of Applied Physiology Respiratory Environmental and Exercise Physiology* 48, 5 (1980), 749–758. https://doi.org/10.1152/jappl.1980.48.5.749
- [11] Mayank Goel, Elliot Saba, Maia Stiber, Eric Whitmire, Josh Fromm, Eric C Larson, Gaetano Borriello, and Shwetak N Patel. 2016. Spirocall: Measuring lung function over a phone call. In Proceedings of the 2016 CHI conference on human factors in computing systems. 5675–5685.
- [12] John L Hankinson, John R Odencrantz, and Kathleen B Fedan. 1999. Spirometric reference values from a sample of the general US population. American journal of respiratory and critical care medicine 159, 1 (1999), 179–187.
- [13] V. Hoffstein and J. J. Fredberg. 1991. The acoustic reflection technique for noninvasive assessment of upper airway area. European Respiratory Journal 4, 5 (1991) 602-611
- [14] A. C. Jackson, J. P. Butler, E. J. Millet, F. G. Hoppin, and S. V. Dawson. 1977. Airway geometry by analysis of acoustic pulse response measurements. *Journal of Applied Physiology Respiratory Environmental and Exercise Physiology* 43, 3 (1977), 523–536. https://doi.org/10.1152/jappl.1977.43.3.523
- [15] Eric C Larson, Mayank Goel, Gaetano Boriello, Sonya Heltshe, Margaret Rosenfeld, and Shwetak N Patel. 2012. SpiroSmart: using a microphone to measure lung function on a mobile phone. In Proceedings of the 2012 ACM Conference on ubiquitous computing. 280–289.
- [16] Giuseppe Liistro, Carl Vanwelde, Walter Vincken, Jan Vandevoorde, Geert Verleden, Johan Buffels, et al. 2006. Technical and functional assessment of 10 office spirometers. Chest 130, 3 (2006), 657–665.
- [17] Ian Marshall. 1992. Acoustic reflectometry with an arbitrarily short source tube. Journal of the Acoustical Society of America 91, 6 (1992), 3558–3564. https://doi.org/10.1121/1.402845
- [18] Ian Marshall, Michael Rogers, and Gordon Drummond. 1991. Acoustic reflectometry for airway measurement. Principles, limitations and previous work. Clinical Physics and Physiological Measurement 12, 2 (1991), 131–141. https://doi.org/10.1088/0143-0815/12/2/002
- [19] Martin R Miller, JATS Hankinson, Vito Brusasco, F Burgos, R Casaburi, A Coates, R Crapo, Pvd Enright, CPM Van Der Grinten, P Gustafsson, et al. 2005. Standardisation of spirometry. European respiratory journal 26, 2 (2005), 319–338.
- [20] Sonja M. Molfenter. 2016. The Reliability of Oral and Pharyngeal Dimensions Captured with Acoustic Pharyngometry. *Dysphagia* 31, 4 (2016), 555–559. https://doi.org/10.1007/s00455-016-9713-y
- [21] NddMedical. [n. d.]. Portable Spirometry Machine & PC Spirometer EasyOne Air. https://nddmed.com/products/spirometers/easyone-air
- [22] Ellie Oostveen, D MacLeod, H Lorino, R Farre, Z Hantos, K Desager, F Marchal, et al. 2003. The forced oscillation technique in clinical practice: methodology, recommendations and future developments. European respiratory journal 22, 6 (2003), 1026–1041.
- [23] Chris Randolph. 2008. Exercise-induced bronchospasm in children. Clinical reviews in allergy & immunology 34, 2 (2008), 205–216.
- [24] Anne-Marie Russell, Huzaifa Adamali, Philip L Molyneaux, Pauline T Lukey, Richard P Marshall, Elisabetta A Renzoni, Athol U Wells, and Toby M Maher. 2016. Daily home spirometry: an effective tool for detecting progression in idiopathic pulmonary fibrosis. American journal of respiratory and critical care medicine 194, 8 (2016), 989–997.
- [25] David Brian Sharp. 2001. Acoustic pulse reflectometry: a review of the technique and some future possibilities. 8th International congress on Sound and Vibration

- (2001), 1067-1074.
- [26] Mary C Townsend, Occupational, and Environmental Lung Disorders Committee. 2011. Spirometry in the occupational health setting—2011 update. Journal of occupational and environmental medicine (2011), 569–584.
- [27] Yu Chih Tung, Duc Bui, and Kang G. Shin. 2018. Cross-platform support for rapid development of mobile acoustic sensing applications. MobiSys 2018 - Proceedings of the 16th ACM International Conference on Mobile Systems, Applications, and Services (2018), 455–467. https://doi.org/10.1145/3210240.3210312
- [28] Jerry A. Ware and Kehti Aki. 1969. Continuous and Discrete Inverse-Scattering Problems in a Stratified Elastic Medium. I. Plane Waves at Normal Incidence. The Journal of the Acoustical Society of America 45, 4 (1969), 911–921. https://doi.org/10.1121/1.1911568
- [29] Ping Zhou, Liu Yang, and Yao-Xiong Huang. 2019. A smart phone based handheld wireless spirometer with functions and precision comparable to laboratory spirometers. Sensors 19, 11 (2019), 2487.
- [30] Fatma Zubaydi, Assim Sagahyroon, Fadi Aloul, Hasan Mir, and Bassam Mahboub. 2020. Using Mobiles to Monitor Respiratory Diseases. In *Informatics*, Vol. 7. MDPI, 56